

Supporting Information

Effect of the Chain Length and Temperature on the Adhesive Properties of Alkanethiol Self-Assembled Monolayers

Hubert Gojzewski^{†‡}, Michael Kappl[§], and Arkadiusz Ptak^{†*}

[†] Institute of Physics, Poznan University of Technology, Piotrowo 3, PL-60965 Poznan, Poland

[‡] Materials Science and Technology of Polymers, MESA⁺ Institute for Nanotechnology, University of Twente, NL-7500 AE Enschede, the Netherlands

[§] Max Planck Institute for Polymer Research, Ackermannweg 10, D-55128 Mainz, Germany

* Corresponding author. E-mail: arkadiusz.ptak@put.poznan.pl

1. Structure-property relationships of 1-tetradecanethiol and 1-hexadecanethiol SAMs on Au(111) at elevated temperatures

CH₃-terminated alkanethiols molecules are found to adopt on Au(111) with the sulfur headgroup ordering into $(\sqrt{3}x\sqrt{3})R30^\circ$ (*R*-rotated to the gold substrate) structure with 0.5 nm distance between the nearest thiol-neighbors.¹ In such a layer the molecules are tilted on the molecular axis by approximately 30° with respect to the normal to the surface.² The structure reveals an area of 0.216 nm² for one molecule (a molecule located in a orthorhombic unit cell).³ This is a maximum molecular packing that can be obtained. Rarely, another saturation coverage, which is *c*(4x2) superlattice of the $(\sqrt{3}x\sqrt{3})R30^\circ$ lattice structure, was observed.⁴⁵ The *c*(4x2) superlattice has a rectangular unit cell with dimension 0.87 nm x 1.00 nm, and is populated by four molecules. It shows the same surface concentration (coverage) as for hexagonal $(\sqrt{3}x\sqrt{3})R30^\circ$ lattice. Densely packed alkanethiol-SAMs contain randomly distributed depressions with an average diameter of several nm.⁴ The depressions, however, are filled with molecules of the same surface reconstruction, chemisorbed on a lower Au terrace; usually one atomic layer or less often two atomic layers below the main Au terrace.

CH₃-terminated alkanethiol-SAMs on Au(111) at elevated temperatures reveal differences as compared to their room temperatures analogues. Ishida *et al.*⁶ investigated 1-tetradecanethiol SAMs on Au(111) at very high temperatures (130°C, 150°C and 180°C) under nitrogen atmosphere. They found that the layer at 130°C was ordered (but no hexagonal $(\sqrt{3}x\sqrt{3})R30^\circ$ phase present) and initially existing depressions were gathered due to the

molecular mobility. At 150°C ordered regions coexisted with desorbed regions, and at 180°C a completely disordered layer was observed. Unfortunately, the authors did not show the value of the melting point for the investigated SAM. We have estimated this value for a 1-tetradecanethiol SAM to be 97°C. The estimation was performed by interpolation of the melting point values of 1-hexanethiol (35°C), 1-octanethiol (54°C), 1-decanethiol (72°C), 1-dodecanethiol SAMs (94°C), 1-hexadecanethiol (100°C) and 1-octadecanethiol SAMs (110°C)⁷⁻⁹ versus the number of carbons in the alkyl chain. McCarley *et al.*⁸ showed for 1-hexadecanethiol SAMs on Au(111) that 2h of annealing at 100°C in air has no effect on molecular structure and ordering, despite elimination of the depressions. Their study showed, however, that the layer melts above 100°C. This is consistent with the thermal stability of 1-octadecanethiol SAMs in UHV, which are stable until approximately 110°C, i.e. decomposition/desorption is not occurring up to this temperature.⁹

2. Au(111) substrates preparation and characterization

80-100 nm thick Au layer (Wieland-Werke AG) was thermally evaporated at a base pressure of $\sim 10^{-6}$ mbar by PVD technique (Edwards, FL400 Auto 306) on freshly cleaved high-grade mica substrates (Ted Pella Inc.). Au@mica substrates were annealed at 550°C for 2 min under a N₂ stream and quenched in air to induce (111) surface reconstruction in the Au layer upon cooling. Prepared substrates were immediately used for SAM chemisorption.

A proper crystallization and surface reconstruction of Au layers was controlled with X-ray diffraction (XRD) and scanning tunnelling microscopy (STM) measurements, respectively (Fig. S1a and S1b). A diffraction peak at $2\Theta = 38.3^\circ$ (Bruker, D8-Advance diffractometer; copper K α radiation with $\lambda = 0.15418$ nm at room temperature) was detected. This diffraction peak corresponds with (111) crystal plane of Au. Atomically flat Au(111) terraces of 50-400 nm in width with 0.24 nm monoatomic steps, were found by STM observation. For ambient STM imaging of Au(111) terraces (and SAMs' structure; see Section 3 below), we used a MultiMode with a NanoScope IIIa controller (Bruker) operated in constant current mode with mechanically cleaved Pt80/20Ir tips. For UHV STM imaging of Au(111) surfaces with atomic resolution, we used an Omicron UHV STM/AFM (Omicron) operated in constant current mode with chemically etched tungsten tips, at the base pressure of 5×10^{-10} mbar and room temperature.

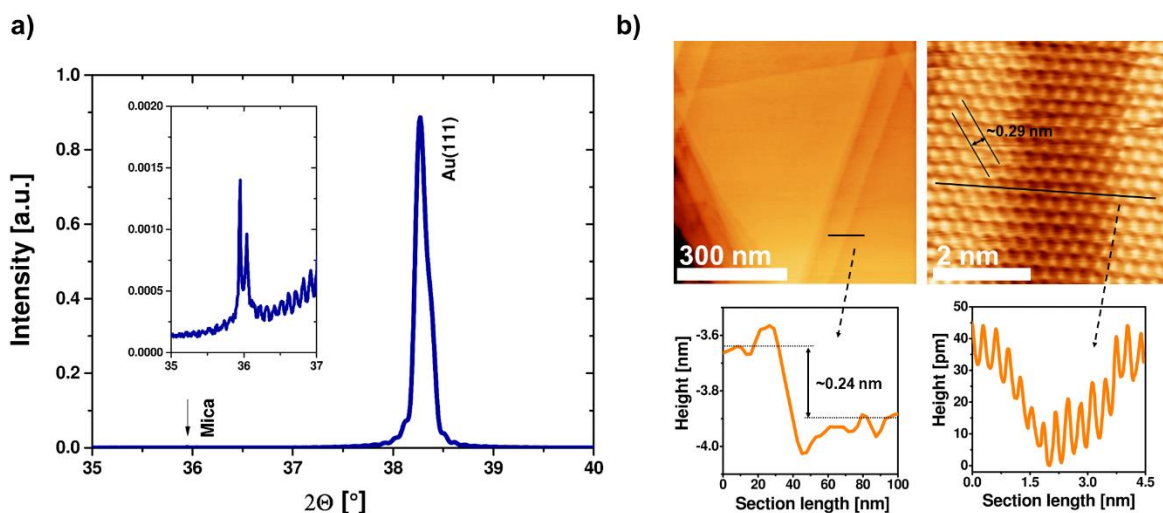


Figure S1. XRD (a) and STM (b) data on Au(111)@mica substrates. The inset in (a) represents a rescaled part of the diffraction plot, indicating the peak from mica (underlying the Au layer). The cross-section plots in (b) show a monoatomic step (left) and the atomic periodicity with a typical herringbone height profile (right).

Potential Au(111) oxidation was analysed by X-ray photoelectron spectroscopy (XPS) performed for the Au(111) substrates with already chemisorbed thiol monolayers (see Section 3, Fig. S3d and S4d).

3. Self-assembled monolayers characterization

Our STM observation at room temperature showed that both types of SAM samples revealed a dominance of the hexagonal $(\sqrt{3}x\sqrt{3})R30^\circ$ lattice structure (Fig. S2). The measurement was repeated after 24h – no structural changes were found in the studied SAMs. Static contact angle was measured using a goniometer (3 μ L water droplets; DataPhysics, model OCA 35). For 1-tetradecanethiol SAMs and 1-hexadecanethiol SAMs we obtained the averaged static contact angle of $(108.6 \pm 0.7)^\circ$ and $(105.4 \pm 0.7)^\circ$, respectively. Comparable values can be found in literature for SAMs of a similar thickness.^{1, 3, 10-12} We repeated the contact angle measurements after 48h to check the stability of the values – no changes beyond the measurement uncertainty (standard deviation) were observed.

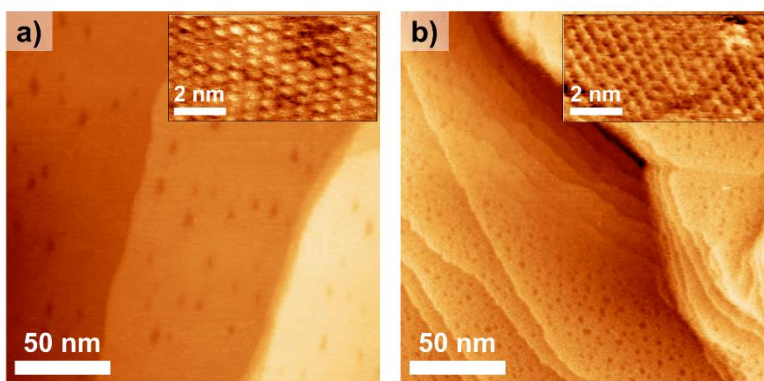


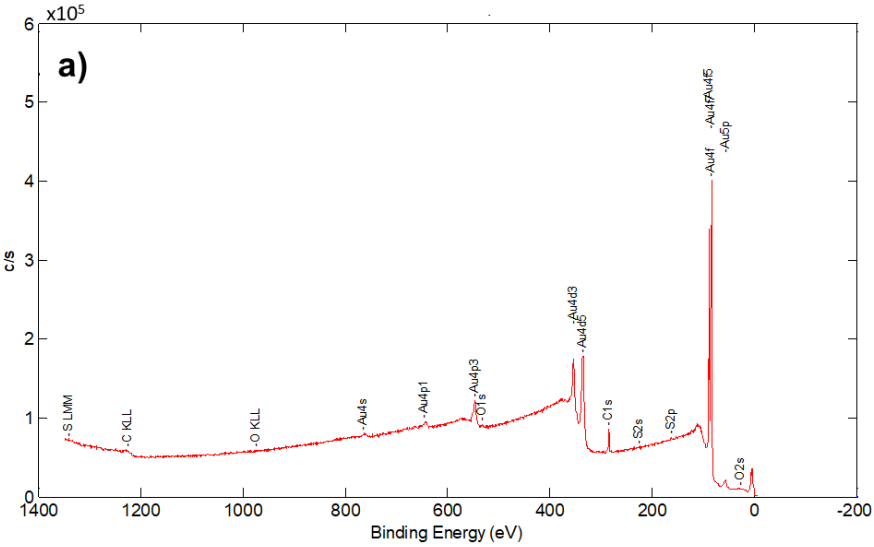
Figure S2. STM data on a 1-tetradecanethiol SAM (a) and a 1-hexadecanethiol SAM (b) on Au(111) substrates. Characteristic depressions are present in both SAMs. The insets show the hexagonal $(\sqrt{3} \times \sqrt{3})R30^\circ$ lattice structure with 0.5 nm of the intermolecular distances.

A set of "twin" SAM samples containing 1-tetradecanethiol and 1-hexadecanethiol, i.e. obtained accordingly to the preparation protocol presented in the manuscript, was analysed by XPS with Quantera SXM (scanning XPS microprobe) from Physical Electronics (aluminum K_α , monochromatic radiation at 1486.6 eV; the base pressure $< 5.4 \times 10^{-10}$ Torr; the detector input angle of 45°). Compass software for XPS control and Multipak v.9.6.1.7 for data reduction were used. The fitting of spectra was mostly performed after shifting of the measured spectra with respect to known reference binding energies. Four spots (200 μm spot size) for each sample were measured, i.e. one for survey XPS spectra (Fig. S3a and S4a) and three for element spectra and their averaging (Fig. S3b-d and S4b-d).

Figures S3 and S4 show a collection of XPS data for 1-tetradecanethiol and 1-hexadecanethiol SAMs on Au(111), respectively. Survey XPS spectra were obtained in three cycles with the pass energy of 224 eV (Fig. S3a and S4a). Typical peaks addressing fractions of Au, O, C, and S are found, from 5 eV to 1345 eV of the binding energy. High-resolution spectra of Au, C, and S are shown in Figures S3b-d and S4b-d and briefly described. The intensity of O1s peaks is low and of minor significance. This small amount of oxygen on the SAM surface is expected as a natural consequence of the sample-air contact (during sample transfers) and the day-light irradiation (photooxidation).¹³ Data in Figures S3b and S4b show that only C-C and C-H carbon components are present in the spectra around 285 eV; these spectra address alkanes.¹⁴ The carbon content is higher for the 1-hexadecanethiol SAM than for the 1-tetradecanethiol SAM sample, indicating differences in the monolayer thickness.

Data in Figs. S3c and S4c show a doublet at around 162.0 eV and 163.2 eV, with the intensity ratio of 2:1, attributed to one sulfur species (thiolate). All fraction of the sulfur is bound to the Au substrate (no peak around 164.5 eV indicating unbound thiols was detected). The sulfur is not oxidized (no peak around 166-170 eV indicating sulfur oxidation was detected).¹⁵ Data in Figs. S3d and S4d show a doublet (right peak – 4f_{7/2} and left peak – 4f_{5/2}) of the Au4f spectral region. The Au surface can be assumed as free of oxygen; the 4f_{7/2} peak is found at around 84 eV whereas for an oxidized Au it would shift to around 85 eV.¹⁶ As expected, the intensity of the 4f_{7/2} peak for the 1-hexadecanethiol SAM is smaller than the intensity of the 4f_{7/2} for the 1-tetradecanethiol SAM due to the difference in the SAM thickness (X-ray absorption).¹⁷ The Au4d_{5/2} and the C1s spectra are shown in Figs. S3e and S4d. They were measured in one plot to find the thickness of the carbon chain layer in SAMs (excluding the sulfur layer). The calculation was performed in the Multipak software.¹⁸ We assumed the carbon chain layer as the polyethylene with its attenuation length of 3.711 nm. The calculation also included the take-off angle (45°) and the intensity of peaks. The calculated thicknesses are as follows: 1.9 nm for the 1-tetradecanethiol SAM and 2.2 nm for the 1-hexadecanethiol SAM. These values are very close to those found in other studies, for instance by Porter *et al.* (ellipsometry).¹⁹

1-tetradecanethiol SAM



Element spectra scans on C, S and Au averaged from 3 randomly chosen acquisition spots:

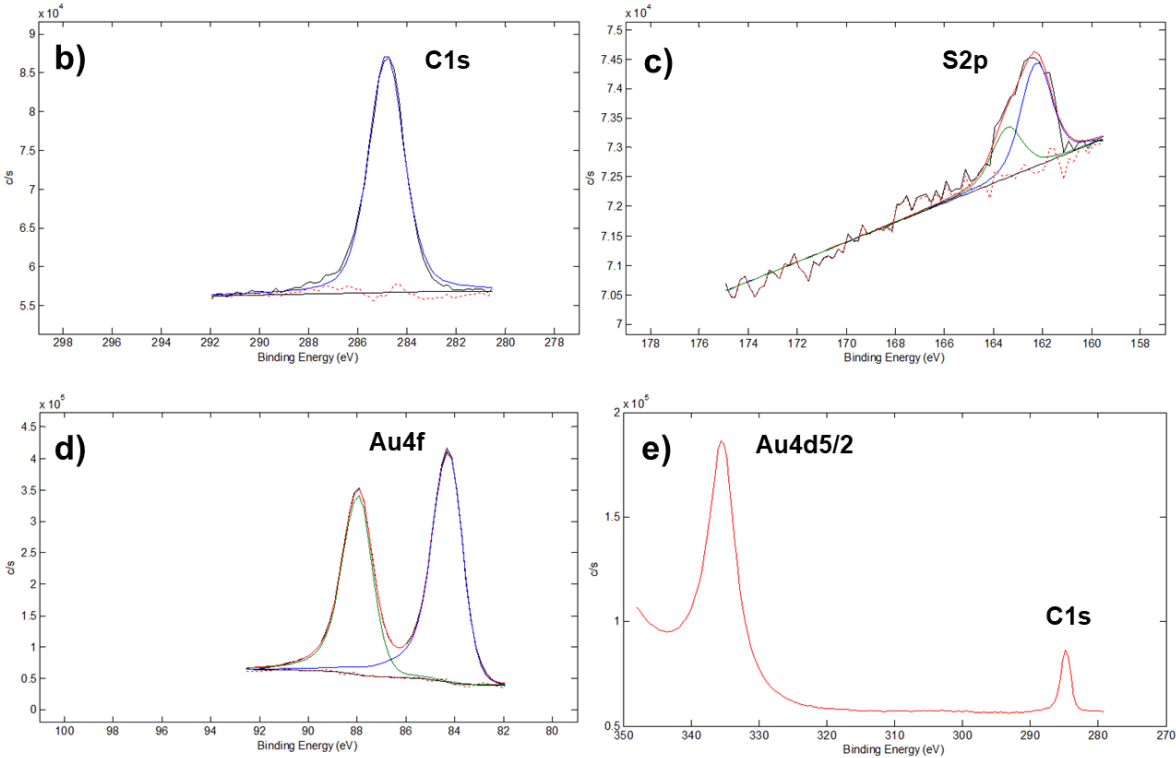
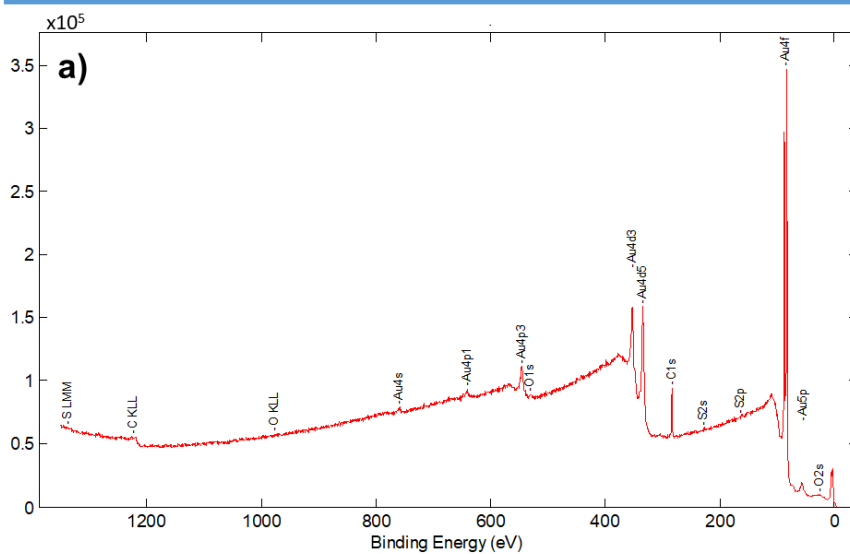


Figure S3. XPS survey spectra (a) and averaged element spectra of C1s (b), S2p (c), Au4f (d), and Au4d5/2 and C1s (e) regions for 1-tetradecanethiol SAM on Au(111).

1-hexadecanethiol SAM



Element spectra scans on C, S and Au averaged from 3 randomly chosen acquisition spots:

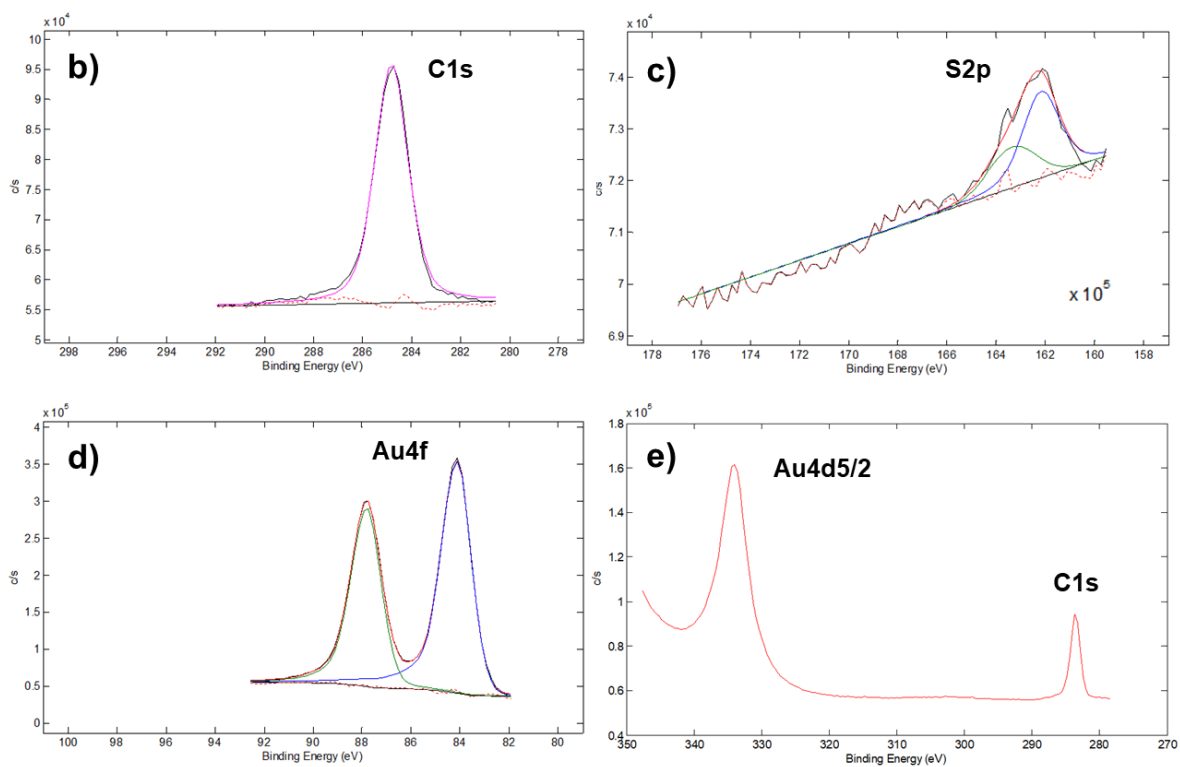


Figure S4. XPS survey spectra (a) and averaged element spectra of C1s (b), S2p (c), Au4f (d), and Au4d5/2 and C1s (e) regions for 1-hexadecanethiol SAM on Au(111).

4. Intermediate results

Table S1. Parameter x_β for the adhesion between a silicon nitride tip and the SAM of:

a) 1-tetradecanethiol

T [°C]	Range of region 2 [nN/s]	x_β [pm]	R^2
25	$8 \cdot 10^3 \div 8 \cdot 10^5$	1.5 ± 0.1	0.94
35	$7 \cdot 10^4 \div 7 \cdot 10^5$	1.6 ± 0.1	0.99
45	$5 \cdot 10^4 \div 1 \cdot 10^6$	2.1 ± 0.8	0.97
55	$2 \cdot 10^5 \div 9 \cdot 10^5$	1.3 ± 0.1	0.99
65	$1.2 \cdot 10^6 \div 2.6 \cdot 10^6$	1.3 ± 0.2	0.99

b) 1-hexadecanethiol

T [°C]	Range of region 2 [nN/s]	x_β [pm]	R^2
25	$6.4 \cdot 10^5 \div 3.4 \cdot 10^6$	0.5 ± 0.1	0.99
35	$3.4 \cdot 10^5 \div 2.4 \cdot 10^6$	1.9 ± 0.1	0.98
45	$4.0 \cdot 10^5 \div 2.3 \cdot 10^6$	1.9 ± 0.7	0.96
55	$9.0 \cdot 10^5 \div 2.3 \cdot 10^6$	1.3 ± 0.1	0.99
65	$1.2 \cdot 10^6 \div 2.6 \cdot 10^6$	1.3 ± 0.2	0.99

R^2 – the coefficient of determination ($R^2 = 1$ for a perfect fit)

Table S2. The minimal adhesion force (F_{ad}^{\min}), the contact area at rupture (A_c), and the number of contacting molecules (N) for the adhesion between a silicon nitride tip and the SAM of:

a) 1-tetradecanethiol

T [°C]	F_{ad}^{\min} [nN]	A_c [nm ²]	N
25	16.8 ± 1.9	345 ± 64	1600 ± 290
35	22.1 ± 1.5	415 ± 64	1900 ± 290

45	26.2 ± 0.9	464 ± 61	2150 ± 280
55	18.6 ± 1.9	370 ± 65	1700 ± 300
65	19.9 ± 0.9	387 ± 54	1800 ± 250

b) 1-hexadecanethiol

T [°C]	F_{ad}^{\min} [nN]	A_c [nm ²]	N
25	8.9 ± 0.1	202 ± 23	940 ± 110
35	9.9 ± 1.2	217 ± 41	1010 ± 190
45	9.3 ± 0.6	209 ± 32	960 ± 150
55	15.4 ± 0.9	292 ± 43	1350 ± 200
65	14.5 ± 1.3	280 ± 47	1300 ± 220

5. Final results

Table S3. The distance between the bound state and an activation barrier on the free-energy interaction potential in the absence of external forces (x_β^*) and the free-energy of activation (ΔG_β^*) for the adhesion between a silicon nitride tip and **a single molecule of:**

a) 1-tetradecanethiol

T [°C]	Range of region 2 [nN/s]	x_β^* [nm]	ΔG_β^* [k _B T]	R^2
25	$7 \cdot 10^3 \div 1 \cdot 10^6$	2.4 ± 0.5	18.2 ± 1.8	0.96
35	$7 \cdot 10^4 \div 1 \cdot 10^6$	5.2 ± 0.8	32.6 ± 3.0	0.98
45	$6 \cdot 10^4 \div 1 \cdot 10^6$	4.8 ± 1.9	28.3 ± 7.3	0.97
55	$1 \cdot 10^4 \div 1 \cdot 10^6$	5.2 ± 0.8	33.0 ± 4.0	0.95
65	$1 \cdot 10^4 \div 1 \cdot 10^6$	5.4 ± 0.6	31.1 ± 2.8	0.96

b) 1-hexadecanethiol

T [°C]	Range of region 2 [nN/s]	x_{β}^* [nm]	ΔG_{β}^* [k _B T]	R^2
25	$5.0 \cdot 10^5 \div 5.6 \cdot 10^6$	4.7 ± 0.2	36.4 ± 1.2	0.91
35	$8.0 \cdot 10^3 \div 4.2 \cdot 10^6$	5.5 ± 0.2	42.0 ± 1.2	0.95
45	$5.0 \cdot 10^4 \div 4.1 \cdot 10^6$	5.3 ± 0.2	37.8 ± 0.8	0.94
55	$1.0 \cdot 10^5 \div 4.1 \cdot 10^6$	6.1 ± 0.4	47.5 ± 4.2	0.97
65	$7.0 \cdot 10^5 \div 4.2 \cdot 10^6$	4.9 ± 1.2	45.1 ± 8	0.67

Acknowledgment

Authors are grateful to Dr. Wojciech Koczorowski for UHV STM measurements of our Au(111)@mica substrates.

References

- (1) Love, J. C.; Estroff, L. A.; Kriebel, J. K.; Nuzzo, R. G.; Whitesides, G. M. Self-assembled monolayers of thiolates on metals as a form of nanotechnology. *Chem. Rev.* **2005**, *105*, 1103-1169.
- (2) Dubois, L. H.; Nuzzo, R. G. Synthesis, structure, and properties of model organic surfaces. *Annu. Rev. Phys. Chem.* **1992**, *43*, 437-463.
- (3) Schreiber, F. Structure and growth of self-assembling monolayers. *Progr. Surf. Sci.* **2000**, *65*, 151-256.
- (4) Delamarche, E.; Michel, B.; Biebuyck, H. A.; Gerber, C. Golden interfaces: The surface of self-assembled monolayers. *Adv. Mater.* **1996**, *8*, 719-729.
- (5) Delamarche, E.; Michel, B.; Kang, H.; Gerber, C. Thermal stability of self-assembled monolayers. *Langmuir* **1994**, *10*, 4103-4108.
- (6) Ishida, T.; Fukushima, H.; Mizutani, W.; Miyashita, S.; Ogiso, H.; Ozaki, K.; Tokumoto, H. Annealing effect of self-assembled monolayers generated from terphenyl derivatized thiols on Au(111). *Langmuir* **2002**, *18*, 83-92.
- (7) Yang, G.; Liu, G. Y. New insights for self-assembled monolayers of organothiols on Au(111) revealed by scanning tunneling microscopy. *J. Phys. Chem. B* **2003**, *107*, 8746-8759.
- (8) McCarley, R. L.; Dunaway, D. J.; Willicut, R. J. Mobility of the alkanethiol-gold(111) interface studied by scanning probe microscopy. *Langmuir* **1993**, *9*, 2775-2777.

- (9) Chandekar, A.; Sengupta, S. K.; Whitten, J. E. Thermal stability of thiol and silane monolayers: A comparative study. *Appl. Surf. Sci.* **2010**, *256*, 2742-2749.
- (10) Arima, Y.; Iwata, H. Effect of wettability and surface functional groups on protein adsorption and cell adhesion using well-defined mixed self-assembled monolayers. *Biomaterials* **2007**, *28*, 3074-3082.
- (11) Imabayashi, S. I.; Gon, N.; Sasaki, T.; Hobara, D.; Kakiuchi, T. Effect of nanometer-scale phase separation on wetting of binary self-assembled thiol monolayers on Au(111). *Langmuir* **1998**, *14*, 2348-2351.
- (12) Meucci, S.; Gabrielli, G.; Caminati, G. Comparative investigation of Langmuir-Blodgett films and self-assembled monolayers on metal surfaces. *Mater. Sci. Eng. C* **1999**, *8-9*, 135-143.
- (13) Rieley, H.; Kendall, G. K.; Zemicael, F. W.; Smith, T. L.; Yang, S. X-ray Studies of Self-Assembled Monolayers on Coinage Metals. 1. Alignment and Photooxidation in 1,8-Octanedithiol and 1-Octanethiol on Au. *Langmuir* **1998**, *14*, 5147-5153.
- (14) Beamson, G.; Briggs, D. *High resolution XPS of organic polymers : the Scienta ESCA300 database*; Wiley: Chichester [England]; New York, 1992.
- (15) Castner, D. G.; Hinds, K.; Grainger, D. W. X-ray Photoelectron Spectroscopy Sulfur 2p Study of Organic Thiol and Disulfide Binding Interactions with Gold Surfaces. *Langmuir* **1996**, *12*, 5083-5086.
- (16) Xue, Y.; Li, X.; Li, H.; Zhang, W. Quantifying thiol-gold interactions towards the efficient strength control. *Nature Commun.* **2014**, *5*, 4348.
- (17) Laibinis, P. E.; Whitesides, G. M.; Allara, D. L.; Tao, Y. T.; Parikh, A. N.; Nuzzo, R. G. Comparison of the structures and wetting properties of self-assembled monolayers of n-alkanethiols on the coinage metal surfaces, copper, silver, and gold. *J. Am. Chem. Soc.* **1991**, *113*, 7152-7167.
- (18) Briggs, D.; Seah, M. P. *Practical Surface Analysis, Auger and X-ray Photoelectron Spectroscopy*; Wiley 1990.
- (19) Porter, M. D.; Bright, T. B.; Allara, D. L.; Chidsey, C. E. D. Spontaneously organized molecular assemblies. 4. Structural characterization of n-alkyl thiol monolayers on gold by optical ellipsometry, infrared spectroscopy, and electrochemistry. *J. Am. Chem. Soc.* **1987**, *109*, 3559-3568.